Compaction of RNA Hairpins and their Kissing Complexes in Native Electrospray Mass Spectrometry

Josephine Abi-Ghanem[1], Clémence Rabin[1], Massimiliano Porrini[1], Frédéric Rosu[2], Valérie Gabelica[1*]

[1] Univ. Bordeaux, CNRS, INSERM, ARNA, UMR 5320, U1212, IECB, F-33600 Bordeaux, France.

[2] Univ. Bordeaux, CNRS, INSERM, IECB, UMS 3033, F-33600 Pessac, France.

SUPPORTING INFORMATION

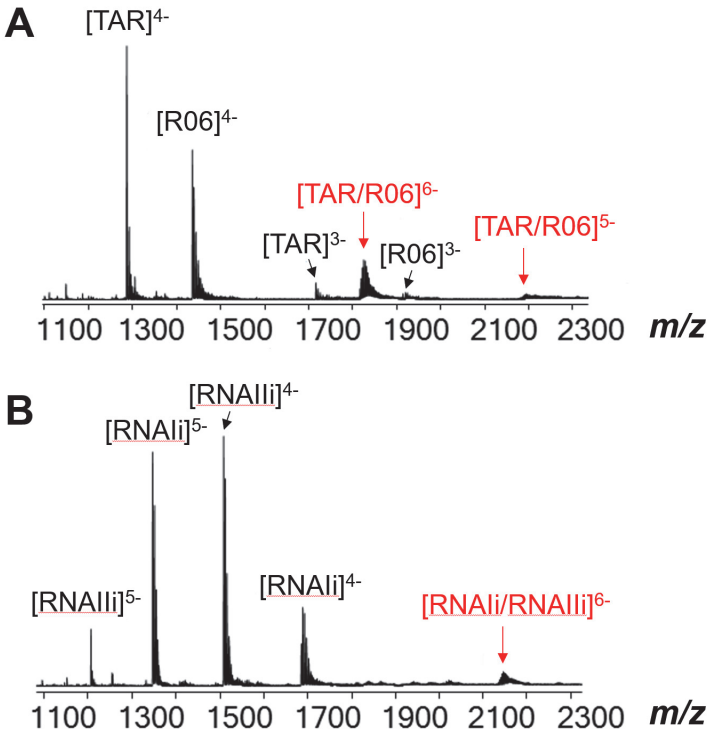

Figure S1: Representative electrospray mass spectra of the hairpins and kissing complexes in soft pre-IMS conditions.

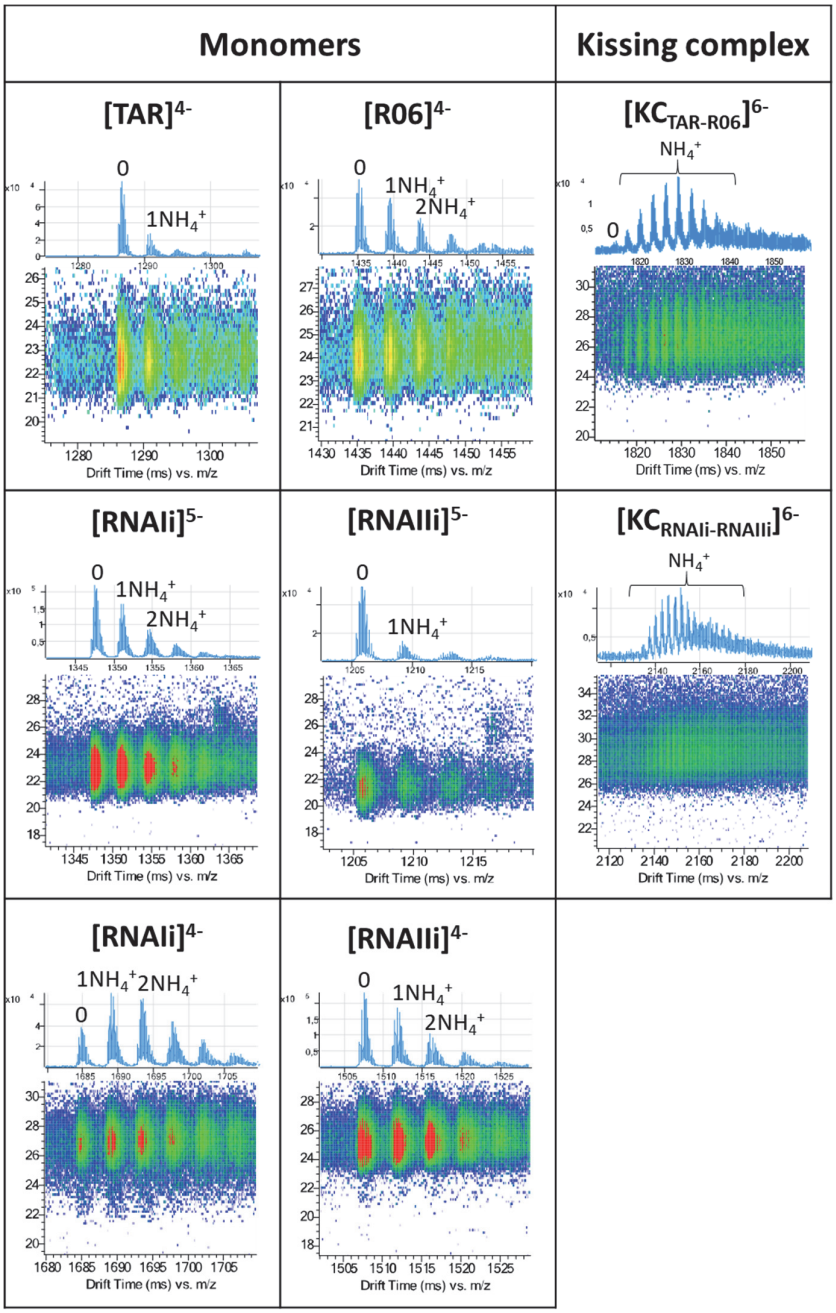

Figure S2: Arrival time distributions of hairpins and kissing complexes using the "soft" tuning parameters (Trap Entrance Grid Delta of 4V and fragmentor set at 350V). The drift time distribution does not depend significantly on the number of ammonium adducts preserved.

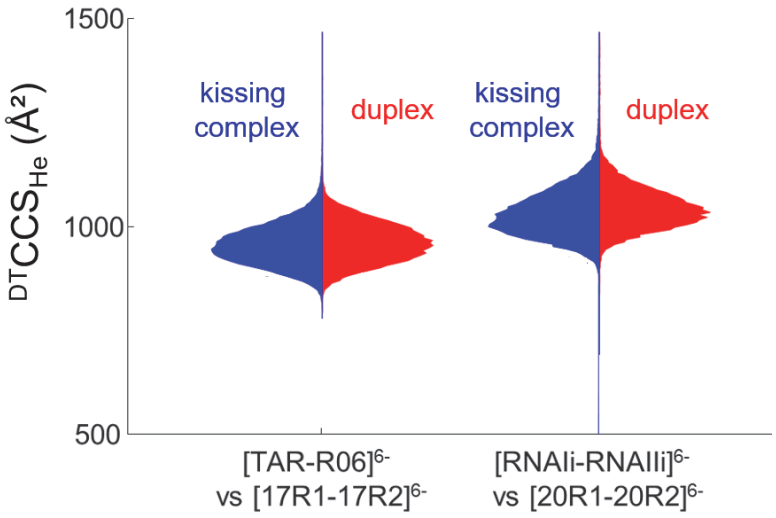

Figure S3: Violin plots comparing the CCS distribution obtained for each kissing complexes and their corresponding duplexes. The sequences of the controls were as follows. 17R1: 5'- GGA GCU CCC AGA CGA CC -3'; 17R2: 5'- GGU CGU CUG GGA GCU CC -3'; 20R1: 5'- GUG AGC UCC CAG ACG ACC UG -3'; 20R2: 5'- CAG GUC GUC UGG GAG CUC AC - 3'.

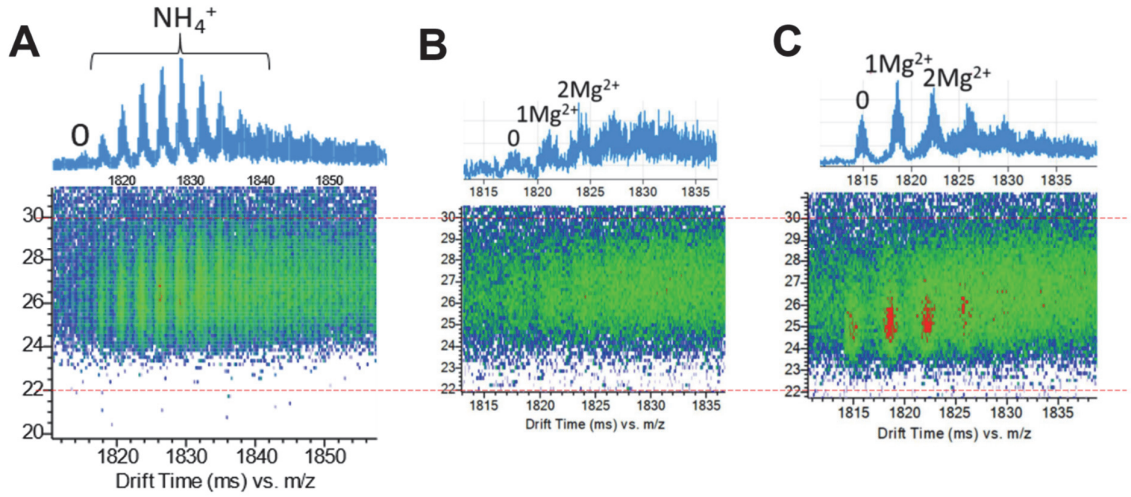

Figure S4: Dependence of the arrival time distribution on the adduct distribution the kissing complex $[TAR:R06]^{6-}$. (A) Recorded from a solution containing 150 mM NH_4AOc, soft conditions as described in the main text; **(B—C)** recorded from a solution containing 150 mM NH_4AOc and 200 µM $Mg(OAc)_2$ (prepared from magnesium acetate tetrahydrate for molecular biology, min 99%, Sigma) in (B) soft conditions as described in the main text and (C) same conditions except the fragmentor voltage = 600 V.

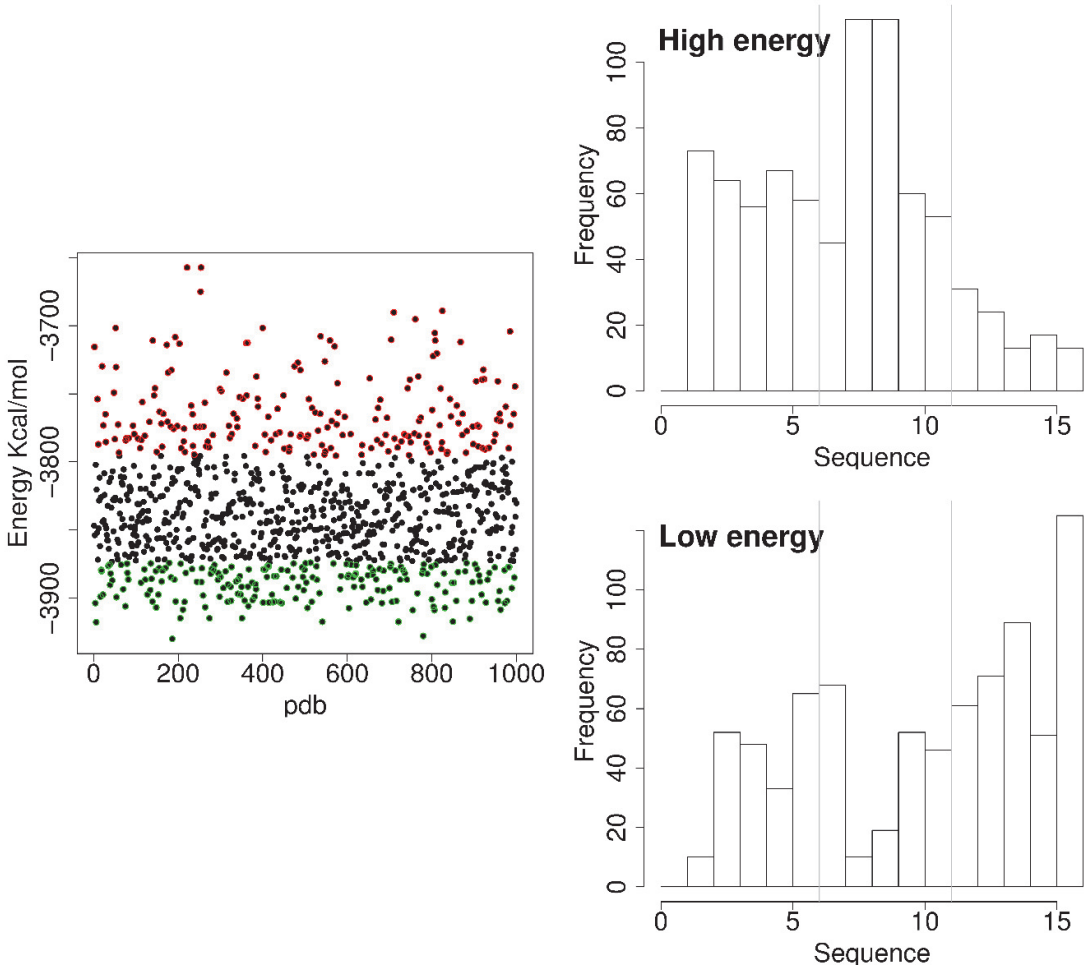

Figure S5: Random protonation scheme and histogram along the sequence for the 200 structures with the lowest energy for $[TAR]^{4-}$. In Panel a) is shown the single point energy calculation on 1000 randomly protonated structures. The red and green dots are the selected 200 structures with the highest and lowest energy respectively and alongside the histogram showing the distribution of the deprotonated residues along the sequence. This histogram with High and Low energy give rise to the Least Probable and Most Probable protonation scheme respectively.

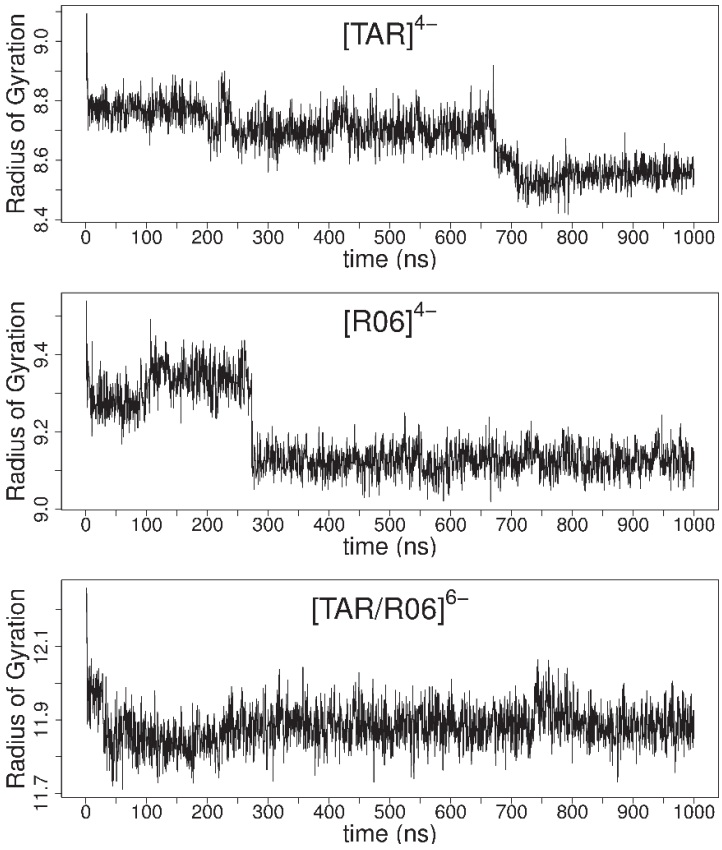

Figure S6: Radius of gyration of the RNA hairpin (TAR , R06) and for the KC TAR/R06 along the MD simulation.

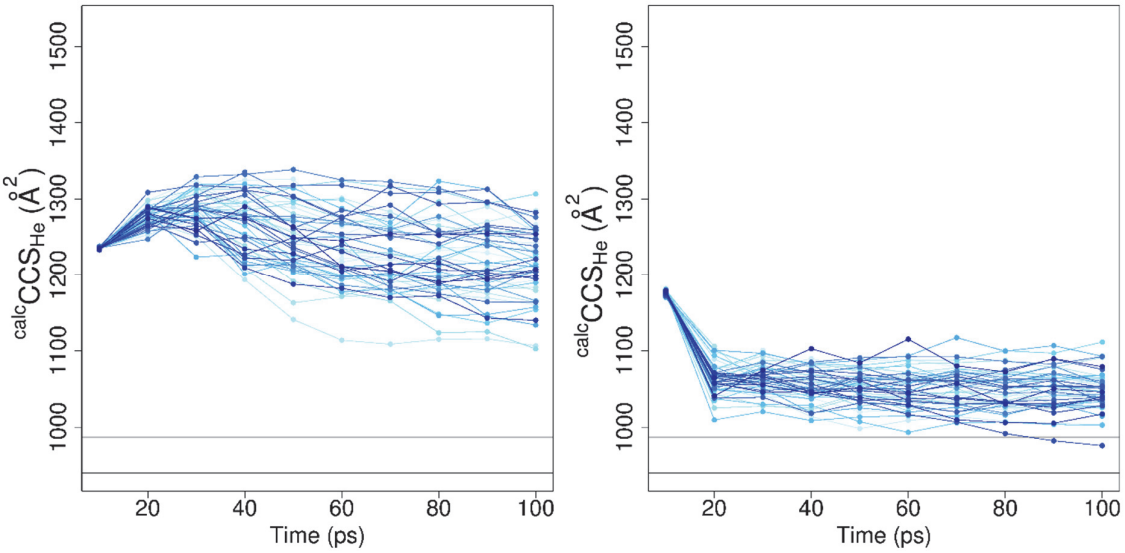

Figure S7: Heating process with and without restraints on the KC [TAR/R06]$^{6-}$. The figure represents the distribution of the CCS along the heating. In the left panel without restraints and in the right panel with restraints. We could observe a drastic compaction during the first step of the heating leading to very compact structures, closer to the experimental ones.

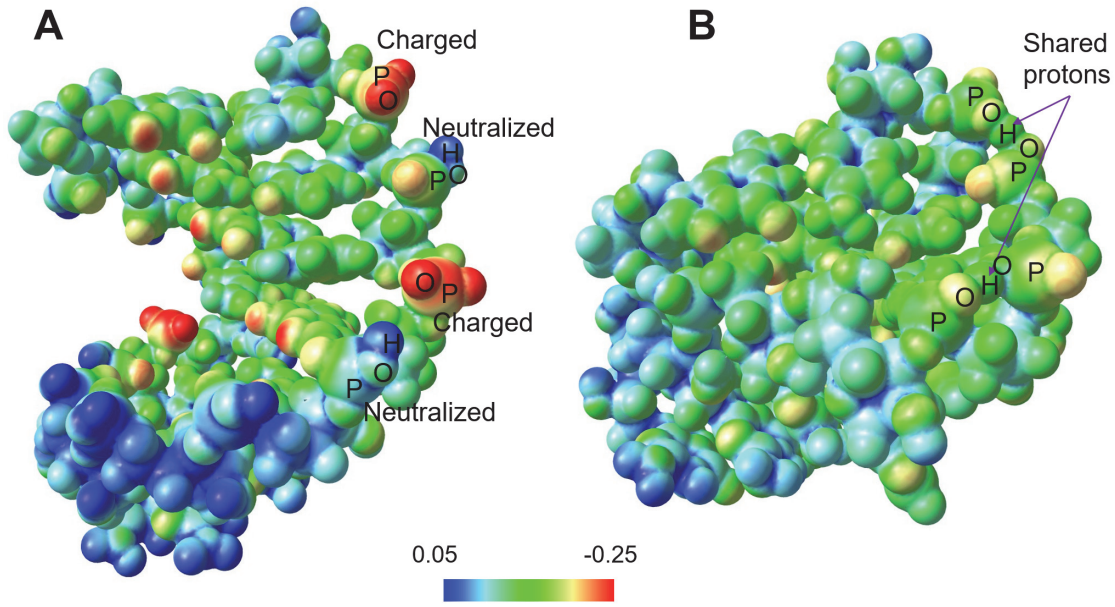

Figure S8: Starting structure (A) and optimized structure (B) of the truncated hairpin TAR14^{3-}. The color coding represents the electrostatic potential calculated from the total electronic density (blue: positive charges; red: negative charges). The phosphate groups neutralized by protons are number 1, 4 and 7 (from the 5'-end).